Polym. Korea, Vol. 50, No. 4, pp. 544-553 (2026)
https://doi.org/10.7317/pk.2026.50.4.544
ISSN 2234-8077(Online)

탄소섬유-카본블랙 상승 전도 네트워크 기반 신축성 전도성 액상 실리콘 고무 복합재료

Xiaoyong Hao†
RONG SHENG Machinery Manufacture Ltd. of Huabei Oilfield, Hebei
(2026년 2월 25일 접수, 2026년 4월 16일 수정, 2026년 4월 28일 채택)

Carbon Fiber-Carbon Black Synergistically Reinforced Liquid Silicone Rubber Composite for Stretchable Conductive Materials

Xiaoyong Hao†
Hebei Huabei Petroleum RONGSHENG Machinery Manufacturing Co., Ltd., Renqiu, Hebei 062550, China
(Received February 25, 2026; Revised April 16, 2026; Accepted April 28, 2026)

Abstract: Flexible and stretchable conductive materials represent an emerging class of advanced functional materials. Among them, rubber–carbon composites have attracted considerable attention for their potential in fabricating flexible, stretchable conductive systems. Carbon fiber (CF), as a representative carbon material, offers advantages such as large aspect ratio and the ability to form effective conductive networks through interconnection. However, commercially available CF is predominantly supplied in bundled form. During compounding with conventional rubber matrices, high shear forces are typically required to achieve uniform dispersion, often leading to severe CF breakage and a consequent decline in the electrical conductivity of the composite. In this study, a low-viscosity, self-crosslinking, two-component room-temperature vulcanizing liquid silicone rubber (LRTV) was employed as the matrix. To overcome the dispersion issues of bundled CF, short-cut CF bundles were treated with air plasma to induce CF fluffing, thereby improving their uniform distribution within the LRTV matrix. Additionally, surface modification of carbon black (CB) with silane coupling agents was performed to eliminate the adverse effect of oxygen-containing functional groups on composites, which had been found to inhibit the self-crosslinking process of LRTV. Using a simple and reliable injection molding process, high-performance flexible and stretchable conductive composites were successfully prepared. The synergistic influence of CF and CB on the electrical conductivity of the composites was systematically investigated. Results showed that the electrical conductivity of the composites was highly sensitive to CF content. At a fixed CB content of 3 wt%, increasing the CF content from 1 wt% to 4 wt% led to a six-fold enhancement in conductivity. In contrast, varying CB content had a minimal impact. At a fixed CF content of 3 wt%, increasing the CB content from 1 wt% to 5 wt% only increased the conductivity by 0.11 S/m. Further studies on the electrical response of the composites under large-strain cyclic deformation revealed that samples with 1 wt% CF and 3 wt% CB exhibited periodic fluctuations in conductivity in response to deformation, demonstrating promising potential for applications in flexible sensors. On the other hand, the composite containing 4 wt% CF and 3 wt% CB exhibited a smooth conductivity profile with minimal variation, indicating its suitability for flexible conductor applications. This work presents a novel strategy for the development of flexible and stretchable conductive electrodes or sensor materials, offering new opportunities in wearable electronics.

Keywords: stretchable conductive, composites, silicone rubber, carbon materials.

Introduction

With the rapid advancement of artificial intelligence, the demand for flexible and stretchable electronic devices has surged, driving their widespread application in modern electronics and related scientific fields.[1-3] Currently, the primary candidates for flexible and stretchable conductive materials are conductive polymer composites, among which rubber–carbon composites have emerged as a research hotspot for the fabrication of such materials.[4-6] Flexible and stretchable conductive materials are defined as materials capable of maintaining high electrical conductivity while undergoing mechanical deformation, particularly stretching.[7] However, most of the existing

†To whom correspondence should be addressed.
772914312@qq.com, ORCID 0009-0006-8113-3332

flexible conductive materials exhibit significant fluctuations in electrical resistance during deformation and fail to retain stable conductivity under large strains. Consequently, the development of simple and reliable fabrication strategies for flexible and stretchable conductive materials—while ensuring stable electrical performance under conditions of large deformation and cyclic strain—remains an urgent challenge that must be addressed.

Most flexible conductive materials are designed for applications involving direct contact with the human body. To minimize the risk of allergic reactions, biocompatible silicone rubber is considered the optimal choice for the matrix material.[8,9] In recent years, numerous studies have employed silicone rubber as a flexible matrix, incorporating carbon fiber (CF), carbon black (CB), and multicomponent fillers as conductive and reinforcing agents to fabricate conductive rubber composites.[10-15] These efforts have yielded promising results and demonstrated significant potential for practical applications.[16] For example, Huang et al. used CF as a conductive filler, adjusted the viscosity of liquid silicone rubber by adding thixotropic agents, and then prepared highly conductive composite materials with oriented carbon fibers using 3D printing technology. Research has shown that the conductive properties of the composite material are superior in the direction parallel to the orientation compared to the direction perpendicular to the orientation.[17] Azizkhani *et al*. used chopped CF as the conductive filler and silicone rubber as the stretchable polymer matrix to prepare a piezoresistive composite strain sensor. Under cyclic tensile conditions with strain amplitudes up to 25%, the composites still exhibit good conductivity.[18] Yang *et al*. dissolved solid silicone rubber in a hexane suspension containing CF/CB, and mechanically stirred to mix silicone rubber, CF, and CB. The hexane was then removed, and the mixture was processed through an open mill into a vulcanization system to prepare a flexible, stretchable conductive composite material. The results showed that the composite material containing 12.5 wt% CB maintained good electrical conductivity even under large deformations.[19] As a carbon-based material, CF offers advantages such as a relatively large aspect ratio and ease of forming interconnected conductive networks. However, commercially available CF is typically supplied in bundled form, and during conventional silicone rubber compounding, high shear forces are required to achieve uniform dispersion. This often results in severe breakage of the CF, thereby significantly compromising the electrical conductivity of the resulting composite.[20,21] Previous studies have attempted to address this issue using conventional silicone rubber solution blending methods. However, such approaches not only introduce the risk of solvent contamination but also necessitate mechanical incorporation of the vulcanization system, which can further exacerbate CF fragmentation.

In this study, bundled short-cut CF were subjected to plasma treatment to induce CF fluffing, while CB particles were surface-modified using a silane coupling agent. A flexible and stretchable conductive composite material based on CF-CB/silicone rubber was subsequently fabricated through simple mechanical mixing and injection molding. The synergistic effects of CF and CB on the electrical conductivity and mechanical properties of the silicone rubber composites were systematically investigated. Furthermore, the electrical conductivity behavior of the composites under cyclic tensile loading within a large strain range was evaluated. This work presents a facile and reliable strategy for the preparation of flexible stretchable conductive materials, enabling the composites to maintain stable electrical conductivity under conditions of significant deformation and alternating strain.

Experimental

Materials. Liquid silicone rubber (Part A and Part B, viscosity: 1.9 Pa.s, industrial grade) purchased from Shenzhen Hongyejie Technology Co., Ltd., China; γ-Methylacryloxypropyl trimethoxysilane (KH-570, analytical grade) purchased from Guangdong Lvwei New Materials Technology Co., Ltd., China; chopped carbon fiber (T700, industrial grade) purchased from Weihai Guangwei Composite Materials Technology Co., Ltd., China; carbon black (industrial grade) purchased from Tianjin Tianyi Century Chemical Products Development Co., Ltd., China; formic acid (analytical grade) purchased from Shanghai Aladdin Bio-Chemical Technology Co., Ltd., China.

Surface Modification of CB and Fluffing Treatment of CF. The pH of the ethanol-water solution was adjusted to 3.5 with formic acid. Subsequently, CB and the silane coupling agent KH-570 were added to the solution and the mixture was allowed to react for 12 h. After the reaction, the mixture was filtered to remove the solvent, and the sample was rinsed with ethanol to eliminate unreacted KH-570 and then with distilled water. Finally, the sample was dried in a vacuum oven at 80 °C until a constant weight is achieved.

Air plasma (PT800, Nanjing Jiayang Engineering Technology Co., Ltd., Nanjing, China) was used to fluff the chopped CF bundles for 5 min at a power setting of 300 W and a working frequency of 20 kHz.

Preparation of CF-CB/Silicone Rubber Flexible Stretchable Composite. The processed CF and CB were weighed according to the ratios specified in Table 1 and added to a mortar along with component A of the silicone rubber. The mixture was ground and stirred for 30 min. Subsequently, component B was added, and the grinding and stirring process was continued for an additional 1 min. The resulting uniformly dispersed mixture was then transferred to an injection molding machine, where samples were prepared via injection molding under the following conditions: injection pressure of 150 bar, injection time of 3 s, holding pressure of 120 s, mold temperature of 85 °C, and barrel temperature of 35 °C. The molded samples were crosslinked and cured for 30 min to obtain the CF-CB/silicone rubber flexible stretchable composite materials. The naming scheme for samples with different component ratios is presented in Table 1. The preparation process of the composite materials and the modification mechanism of CB are illustrated in Figure 1.

Table 1. Experimental Formulations of Flexible Stretchable Conductive Composites

Number	CB (wt%)	CF (wt%)	Component A	Component B
#1	1	3	50	50
#2	2	3	50	50
#3	3	3	50	50
#4	4	3	50	50
#5	5	3	50	50
#6	3	1	50	50
#7	3	2	50	50
#8	3	3	50	50
#9	3	4	50	50

Characterization. All experiments were performed in triplicate to ensure statistical reliability. The data are presented as mean ± standard deviation, and the error bars in all figures represent the standard deviation of three independent measurements.

Analysis of Functional Groups and Chemical Elements on the Surface of CB: Fourier transform infrared spectroscopy (FTIR, IS50, Thermo Scientific, USA) was employed to analyze the chemical functional groups present on the surface of CB Prior to analysis, the CB samples—both before and after surface modification—were ground into fine powder, dried, and thoroughly mixed with potassium bromide (KBr) in an agate mortar. The mixture was then compressed into pellets using a pellet press. These pellets were placed under the FTIR spectrometer probe for scanning, with a spectral range of 500–4000 cm^{-1}. X-ray photoelectron spectroscopy (XPS, Thermo Scientific ESCALAB XI+, USA) was utilized to characterize the elemental composition of CB surfaces before and after modification, enabling the identification of surface functional groups. Thermogravimetric analysis (TGA, 209F3, NETZSCH, Germany) was conducted at a heating rate of 10 °C/min to investigate the compositional changes of CB before and after surface.

CF-CB/Silicone Rubber Flexible Stretchable Composites Mechanical Properties Analysis: The mechanical properties of the CF–CB/silicone rubber flexible stretchable composite materials were evaluated using a universal testing machine (Instron-3365, Instron, USA), in accordance with the standard

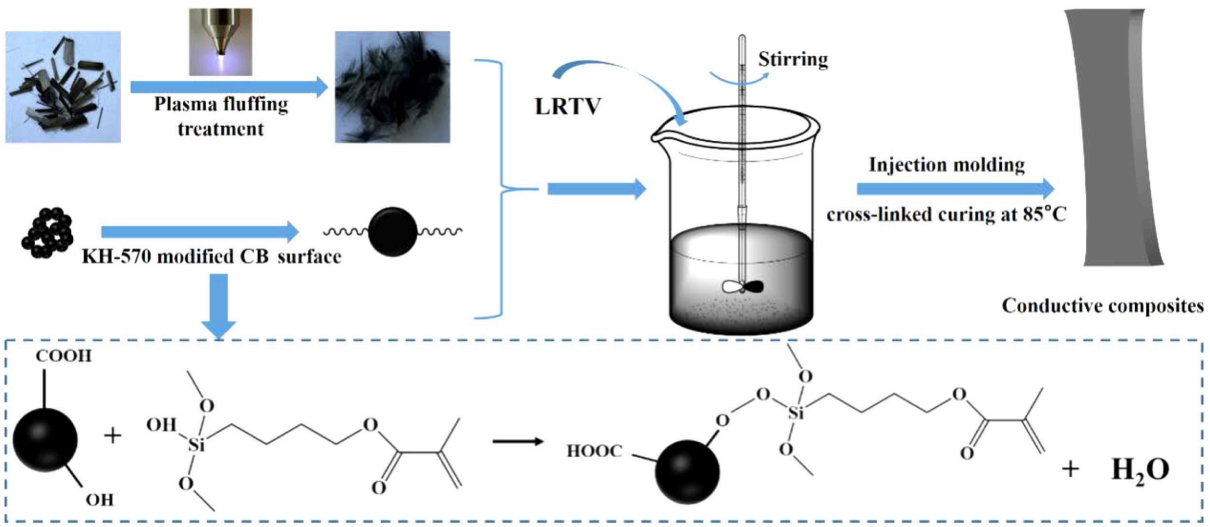

Figure 1. Preparation process of flexible stretchable conductive composite materials and CB surface modification mechanism.

GB/T 528-2009. Dumbbell-shaped tensile specimens were used, and the crosshead speed was set to 500 mm/min. Shore A hardness was measured following the national standard GB/T 531.1-2008.

CF-CB/Silicone Rubber Flexible Stretchable Composites Conductivity Analysis. A sample with dimensions of 12.5 × 12.5 × 2 mm was placed between two copper plates. The working and counter electrodes of the electrochemical workstation (CHI760e, Shanghai Chenhua Instrument Co., Ltd., China) were connected to the respective copper plates. A voltage of 1 V was applied across the material, and the instantaneous current of the CF–CB/silicone rubber composite was recorded using the electrochemical workstation. The electrical conductivity was then calculated using the following formula.

$$\sigma = \frac{I \times L}{U \times S} \quad (1)$$

In the formula: L represents the thickness of the sample (m); S: denotes the contact area between the sample and the electrode plate (m^2); I is the current passing through the composite material (A); U is the applied voltage (V).

CF-CB/Silicone Rubber Flexible Stretchable Composites Swelling Performance Analysis: Take a clean sample and accurately record its initial mass, denoted as m_1. Immerse the sample in toluene for 72 h. After removal, gently wipe off any residual toluene from the sample surface and accurately measure its final mass, denoted as m_2. The mass change rate (S) of the sample is then calculated using the following formula.

$$S = \frac{m_2 - m_1}{m_1} \times 100\% \quad (2)$$

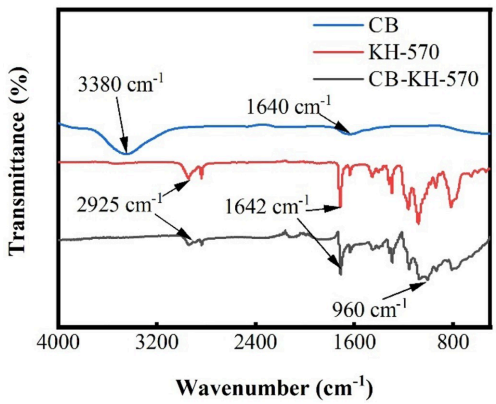

Figure 2. FTIR of CB and CB modified by KH-570.

Results and Discussion

Analysis of Functional Groups and Chemical Elements on the Surface of CB. Infrared spectroscopy was employed to analyze the surface functional group structures of the modified CB Figure 2 presents the infrared spectra of both unmodified and modified CB In the spectrum of the unmodified CB, a strong absorption peak appears at 3380 cm^{-1}, corresponding to the stretching vibration of hydroxyl groups, and a characteristic absorption peak of C=O is observed at 1642 cm^{-1}. The presence of hydroxyl groups is known to hinder the crosslinking of silicone rubber. After surface modification, the hydroxyl peak on the CB surface disappears, and a new absorption peak emerges at 960 cm^{-1}, corresponding to the stretching vibration of the Si–O bond. Additionally, a new peak at 2925 cm^{-1} is attributed to the vibrational absorption of the $–CH_2$ groups from the silane coupling agent. These FTIR results confirm the successful grafting of KH-570 onto the CB surface.

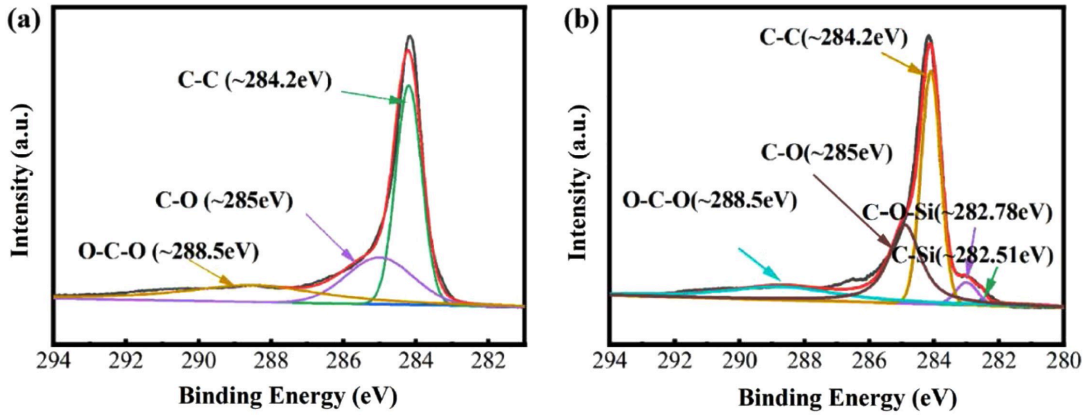

Figure 3. XPS spectra before and after surface modification of CB: (a) C1s spectrum of CB; (b) C1s spectrum of CB-KH-570.

To further verify the successful surface modification of CB by KH-570, XPS was conducted to analyze the surface chemical composition of CB prior to modification, with peak deconvolution performed on the C1s spectrum, as shown in Figure 3(a). The binding energies at 288.5, 285, and 284.2 eV correspond to O–C=O, C–O, and C–C functional groups, respectively. The XPS spectrum of CB after KH-570 modification is shown in Figure 3(b). As illustrated, new binding energy peaks appear at 282.51 eV and 282.78 eV, which are attributed to the C–Si and C–O–Si functional groups, respectively. These results confirm that KH-570 has been successfully grafted onto the surface of CB.

The two-component LRTV used in this study cures via a platinum-catalyzed hydrosilylation reaction between vinyl groups in Component A and hydrosilane groups in Component B. Unmodified CB contains a large number of surface hydroxyl (-OH) and carboxyl (-COOH) groups, as confirmed by the FTIR peaks at 3380 and 1642 cm^{-1}. These oxygen-containing functional groups can coordinate with the platinum catalyst, forming stable complexes that poison the catalyst and reduce its catalytic activity. This leads to incomplete crosslinking of the silicone rubber matrix and a decrease in the mechanical and electrical properties of the composites.

After modification with KH-570, the silane coupling agent undergoes hydrolysis and condensation reactions with the hydroxyl groups on the CB surface, forming covalent Si-O-C bonds. This is evidenced by the disappearance of the hydroxyl peak at 3380 cm^{-1} in the FTIR spectrum and the appearance of C-Si and C-O-Si peaks at 282.51 and 282.78 eV in the XPS spectrum. The grafted KH-570 molecules not only eliminate the catalyst-poisoning sites on the CB surface but also introduce methacryloxy groups that have good compatibility with the silicone rubber matrix. This improves the dispersion of CB in the LRTV matrix and promotes the uniform crosslinking of the silicone rubber, thereby enhancing the overall performance of the composites.

TG Analysis Before and After Surface Modification of Carbon Black. While XPS and FTIR analyses can confirm the presence of KH-570 on the surface of CB, they cannot distinguish whether KH-570 is chemically bonded to the surface or merely physically adsorbed. Therefore, thermogravimetric analysis (TGA) was conducted on CB before and after surface modification. Figure 4 presents the TGA curves of CB prior to and following surface treatment. The boiling point of KH-570 is 250 °C. As shown in the figure, a slight weight loss is observed below 250 °C, which is attributed to the evaporation of residual moisture and the desorption of physically adsorbed KH-570. A more pronounced weight loss occurs between 300 °C and 450 °C, corresponding to the thermal degradation of KH-570 that is chemically grafted onto the CB surface. This significant mass loss in the higher temperature range confirms the formation of chemical bonds between KH-570 and the CB surface.

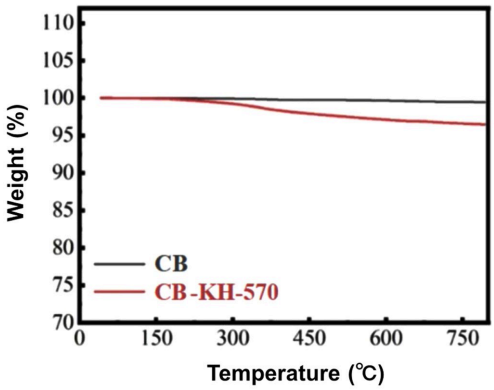

Figure 4. TG curves of CB and CB-KH-570.

CF-CB/Silicone Rubber Flexible Stretchable Composite Material Internal Microstructure Analysis. Figure 5 illustrates the microstructure of the CF-CB/silicone rubber flexible stretchable conductive composite material. As shown, the transparency of the composite material decreases progressively with increasing CB content. When the CB content reaches 3 wt%, only a faint outline of the CF is visible, and CB particles begin to exhibit aggregation within the composite matrix. Figure 5(f) presents a color-adjusted image of sample #6 (1 wt% CF, 3 wt% CB), in which only CF is retained. The image reveals that CF, after plasma-induced fluffing, is uniformly dispersed throughout the composite, with individual fibers separated and interwoven, effectively avoiding the formation of fiber bundles. This indicates that plasma fluffing significantly enhances CF dispersion. Furthermore, individual CF are interconnected by CB particles, which act as a bridging framework within the network, synergistically forming a conductive network with CF.

CF-CB/Silicone Rubber Flexible Stretchable Composites Mechanical Properties Analysis. Figure 6 presents the mechanical properties of composite materials with a fixed CF content of 3 wt% and varying CB content. As shown in Figure 6(a) and 6(b), the tensile strength of the composite gradually increases with increasing CB content and eventually stabilizes, while the elongation at break remains largely unchanged. Meanwhile, the permanent deformation of the composite material continues to

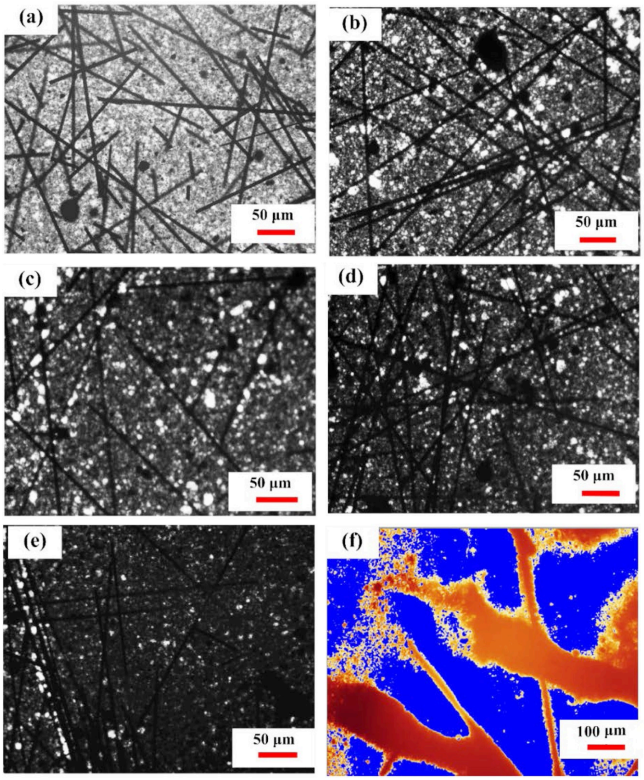

Figure 5. Microscopic morphology of composites: (a) #1: 3 wt% CF 1 wt% CB; (b) #2: 3 wt% CF 2 wt% CB; (c) #6: 1 wt% CF 3 wt% CB; (d) #9: 4 wt% CF 3 wt% CB; (e) #5: 1 wt% CF 3 wt% CB; (f) Microscopic photo with color grading showing #6: 1 wt% CF 3 wt% CB.

rise with increasing amounts of modified CB This phenomenon can be attributed to the fact that the addition of modified CB restricts the movement of the silicone rubber molecular chains. During the tensile process, the modified CB particles undergo relative displacement, occupying the original positions of the molecular chains and preventing them from returning to their initial configurations. As a result, the permanent deformation of the material increases.

Figure 7 illustrates the mechanical properties of composite materials with a fixed CB content of 3 wt% and varying CF contents. As shown in Figure 7(a), the stress–strain curves indicate that the mechanical properties of the composite materials exhibit a decreasing trend with increasing CF content. Furthermore, as seen in Figure 6 and 7, when CF and CB are used in combination to reinforce silicone rubber composites, the mechanical properties are predominantly influenced by CB This is because CF possesses high rigidity and modulus, while the interfacial strength between CF and the flexible polymer matrix is relatively low, making the interface susceptible to stress concentration. Under external loading, such stress concentration leads to premature failure of the composite, thereby reducing its tensile strength. As shown in Figure 7(d), the permanent deformation of the composite material increases with rising CF content. When the CF content reaches 4 wt%, the

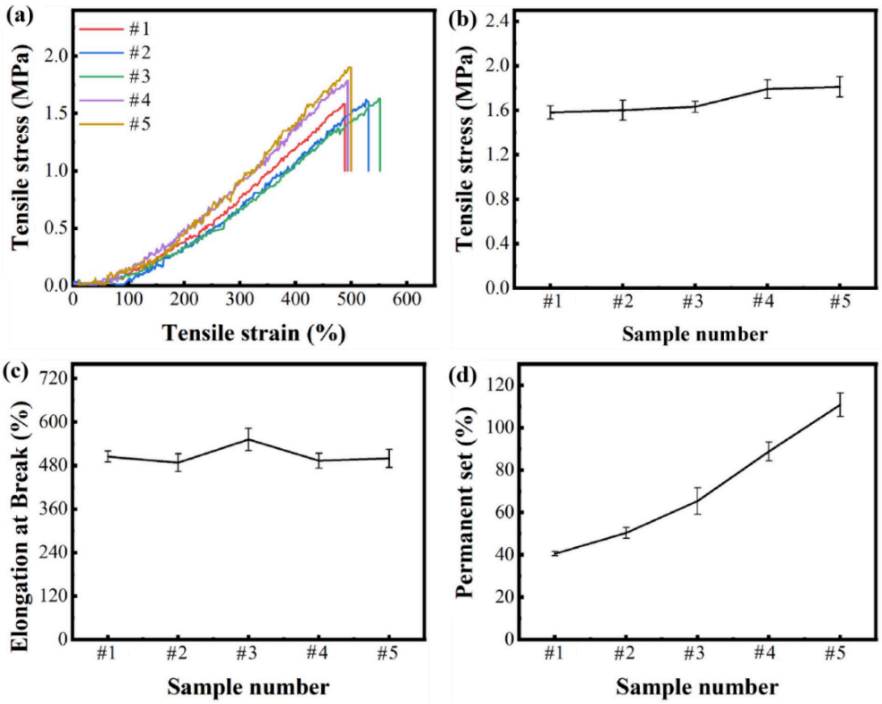

Figure 6. Mechanical properties of composites with fixed CF content and variable CB content: (a) stress-strain curve; (b) tensile strength; (c) elongation at break; (d) permanent deformation.

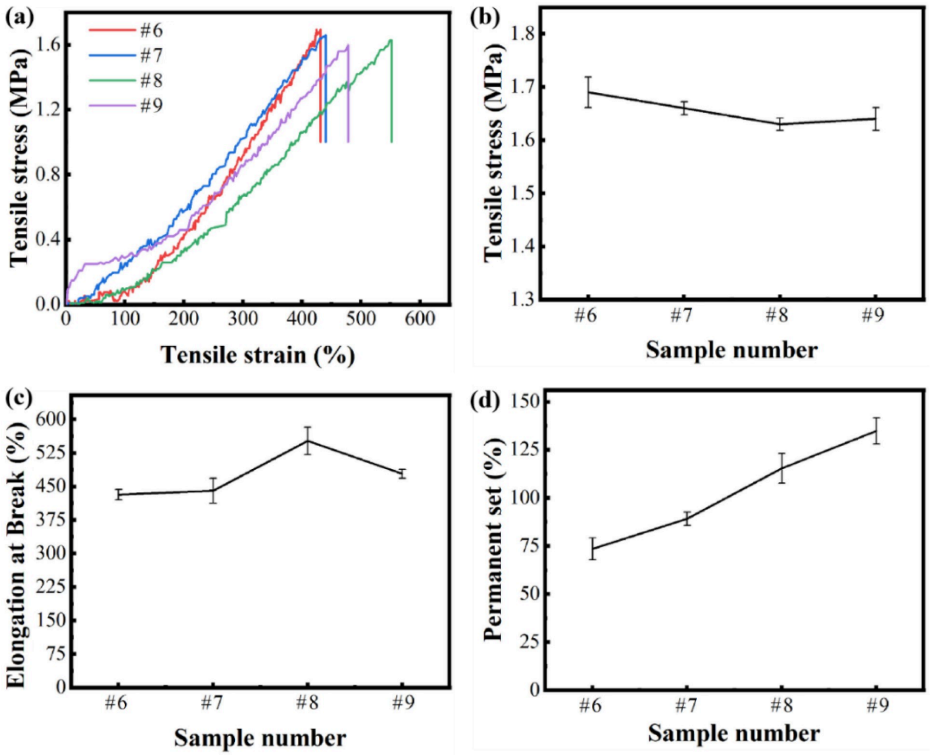

Figure 7. Mechanical properties of composites with fixed CB content and variable CF content: (a) stress-strain curve; (b) tensile strength; (c) elongation at break; (d) permanent deformation.

permanent deformation is twice that observed at 1 wt%. Upon unloading, the silicone rubber molecular chains tend to revert to a low-energy state characterized by a coiled conformation. However, the incorporation of rigid CF restricts the mobility of these chains, preventing them from returning to their original configurations and thus resulting in greater permanent deformation. As CF content increases further, the hindrance to molecular chain recovery becomes more pronounced, leading to a corresponding increase in the permanent deformation of the composite material.

Figure 8 presents the electrical conductivity of composite materials with varying CF and CB contents. As shown in Figure 8(a), when the CF content is fixed at 3 wt%, the electrical conductivity of the composite material increases gradually with increasing CB content, though the overall improvement is relatively modest. Specifically, the addition of 5 wt% CB results in a 26.8% increase in electrical conductivity compared to 1 wt% CB. In contrast, as shown in Figure 8(b), when the CB content

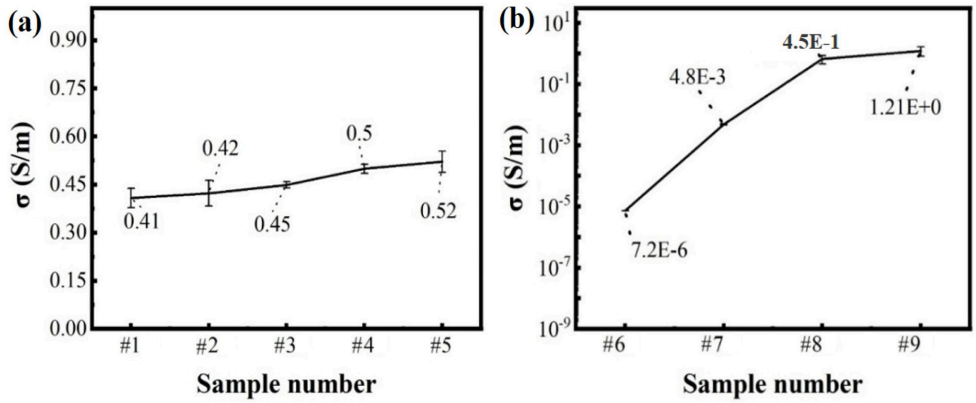

Figure 8. Electrical conductivity of composite materials from different samples.

is fixed at 3 wt%, the electrical conductivity of the composite material increases dramatically with increasing CF content—from 7.2×10^{-6} S/m at 1 wt% CF to 1.21 S/m at 4 wt% CF—representing an enhancement of six orders of magnitude. This significant improvement is attributed to the morphological differences between CF and CB. Due to the small particle size and relatively large inter-particle gaps, CB alone contributes minimally to conductivity. In comparison, CF offers longer and more continuous conductive pathways, facilitating more efficient electron transport. Furthermore, a synergistic conductive effect is observed between the interlaced CF and the dispersed CB within the composite matrix. CF acts as an extended conductive bridge, connecting isolated CB particles, while the interaction between these two conductive components contributes synergistically to the enhanced electrical performance of the composite material.

Figure 9 illustrates the electrical conductivity of the composite material under cyclic tensile loading at a strain of 20%, investigating the synergistic effect between CF and CB on electrical conductivity under repeated deformation. Figure 9(a) shows the conductivity response of the composite containing 1 wt% CF and 3 wt% CB. As observed, the relative resistance change ($\Delta R/R_0$) exhibits periodic fluctuations corresponding to the cyclic tensile strain, along with significant variations. A "shoulder" phenomenon appears during the initial cycles, which is consistent with the findings reported by Yang *et al*., who attributed this behavior to the destruction and reconstruction of the conductive network.[19] The "shoulder" phenomenon observed during the initial strain cycles can be attributed to the sequential microstructural evolution of the conductive network. In the first stage of stretching, the loosely connected CB particles that are only in physical contact with each other and with CFs are the first to separate, leading to a rapid increase in electrical resistance. As the strain continues to increase, the weak overlapping points between adjacent CFs begin to break, further increasing the resistance. However, simultaneously, the CFs undergo gradual alignment along the stretching direction, and the CB particles slide and redistribute on the surface of the aligned CFs. This redistribution allows CB particles to form new conductive bridges between adjacent CFs, which slows down the rate of resistance increase and results in the characteristic "shoulder" in the resistance-strain curve. After several loading-unloading cycles, the conductive network reaches a dynamic equilibrium state, and the "shoulder" phenomenon gradually disappears. Moreover, changes in the local static electric field during repeated strain cycles are considered another contributing factor to the emergence of the shoulder feature. These periodic variations in conductivity under mechanical strain indicate that the composite has considerable potential for application in flexible sensing technologies. Figure 9(b) displays the conductivity response of a composite material with 4 wt% CF and 3 wt% CB under the same cyclic strain conditions. In this case, the relative resistance change ($\Delta R/R_0$) remains stable throughout the cycles, with the relative resistance change ($\Delta R/R_0$) curve exhibiting minimal fluctuation and a smooth, flat trend. After 16 loading cycles, the relative resistance change ($\Delta R/R_0$) increases by only 0.02, indicating excellent electrical stability. This enhanced performance is attributed to the higher CF content, where the fibers interlock and synergize with the dispersed CB to form a robust and stable conductive network. These results demonstrate the composite's strong potential for use in flexible conductive applications.

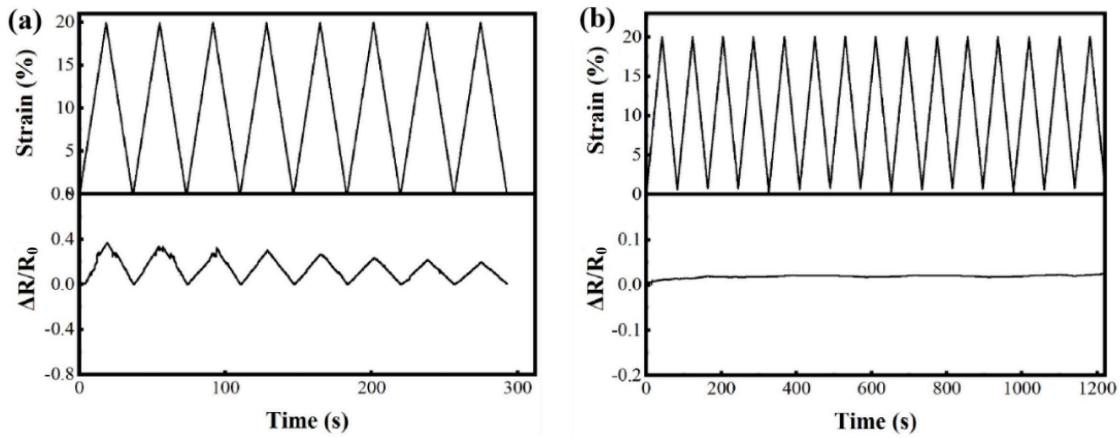

Figure 9. Electrical conductivity of composite materials under cyclic tension: (a) #6: 3 wt% CB 1 wt% CF; (b) #9: 3 wt% CB 4 wt% CF.

Conclusions

By investigating the effects of CB and CF content on the performance of the composite materials, it was found that CF and CB exhibit a synergistic effect in enhancing the electrical conductivity of the composites. The larger-sized CF serves as efficient conductive pathways within the composite, while the smaller-sized CB functions as a hub that interconnects these pathways. The study revealed that the electrical conductivity of composite sample #9 (4 wt% CF, 3 wt% CB) reached 1.21 S/m. Conductive performance is significantly influenced by CF content. When the CB content was fixed at 3 wt%, increasing the CF content from 1 wt% to 4 wt% led to an improvement in electrical conductivity by six orders of magnitude. In contrast, the electrical conductivity was less sensitive to changes in CB content. At a constant CF content of 3 wt%, increasing the CB content from 1 wt% to 5 wt% resulted in a relatively small increase in electrical conductivity—only 0.11 S/m. Additionally, composite sample #6 (1 wt% CF, 3 wt% CB) exhibited significant variation and periodicity in electrical conductivity under deformation, indicating promising potential for application in strain-responsive sensors. On the other hand, composite sample #9 maintained stable electrical conductivity under cyclic strain, characterized by a smooth conductivity curve with minimal fluctuation, highlighting its strong potential for application in flexible conductors.

The optimal compositions for different applications are determined by the structural characteristics of the synergistic conductive network formed by CF and CB For flexible conductor applications, the 4 wt% CF, 3 wt% CB composition is optimal because the high CF content forms a dense, interlocked three-dimensional conductive skeleton. The CB particles fill the gaps between CFs and act as “conductive bridges” to connect adjacent CFs, resulting in a robust conductive network that is resistant to structural damage under cyclic deformation. For strain sensor applications, the 1 wt% CF, 3 wt% CB composition is ideal because the sparse CF network forms a discontinuous conductive pathway. Under mechanical deformation, the weak contact points between CFs and between CFs and CB particles are easily broken and reconnected, leading to significant and periodic changes in electrical conductivity, which is essential for high-sensitivity strain sensing.

Acknowledgements: This work was supported by the National Natural Science Foundation of China Project (No. 52173101), Shandong Provincial Natural Science Foundation Key Project (No. ZR2020KE037), Qingdao City Science and Technology for the People Demonstration and Guidance Special Project (22-3-7-cspz-18-nsh), Shandong Province Postdoctoral Innovation Project (202103024), “Taishan Scholar” Construction Project Special Funding Support and China Postdoctoral Science Foundation (Certificate Number: 2023M733754).

Conflict of Interest: The authors declare that there is no conflict of interest.

References

1. Yang, Y.; Deng, H.; Fu, Q. Recent Progress on PEDOT:PSS Based Polymer Blends and Composites for Flexible Electronics and Thermoelectric Devices. *Mater. Chem. Front*. **2020**, 4, 3130-3152.
2. Zhang, F.-T.; Xu, L.; Chen, J.-H.; Zhao, B.; Fu, X.-Z.; Sun, R.; Chen, Q.; Wong, C.-P. Electroless Deposition Metals on Poly(dimethylsiloxane) with Strong Adhesion As Flexible and Stretchable Conductive Materials. *ACS Appl. Mater. Interfaces* **2018**, 10, 2075-2082.
3. Amjadi, M.; Turan, M.; Clementson, C. P.; Sitti, M. Parallel Microcracks-based Ultrasensitive and Highly Stretchable Strain Sensors. *ACS Appl. Mater. Interfaces* **2016**, 8, 5618-5626.
4. Tee, B. C. K.; Ouyang, J. Y. Soft Electronically Functional Polymeric Composite Materials for a Flexible and Stretchable Digital Future. *Adv. Mater.* **2018**, 30, 1802560.
5. Xu, D.; Wang, Q.; Feng, D.; Liu, P. Facile Fabrication of Multifunctional Poly(ethylene-co-octene)/Carbon Nanotube Foams Based on Tunable Conductive Network. *Ind. Eng. Chem. Res*. **2020**, 59, 1934-1943.
6. Markov, A.; Wördenweber, R.; Ichkitidze, L.; Gerasimenko, A.; Kurilova, U.; Suetina, I.; Mezentseva, M.; Offenhäusser, A.; Telyshev, D. Biocompatible SWCNT Conductive Composites for Biomedical Applications, *Nanomaterials*, **2020**, 10, 2492.
7. Chang, M.; Li, Y.; Xu, L.; Wang, W.; Wang, C.; Wang, R. A Novel Assembled Carbon Black/carbon Nanotubes (CB/MWCNT) Nano-structured Composite for Pressure-sensitive Conductive Silicon Rubber (SR). *J. Mater. Sci.: Mater. Electron*. **2018**, 29, 2716-2724.
8. Chen, Y.-F.; Huang, M.-L.; Cai, J.-H.; Weng, Y.-X.; Wang, M. Piezoresistive Anisotropy in Conductive Silicon Rubber/multi-walled Carbon Nanotube/nickel Particle Composites via Alignment of Nickel Particles. *Compos. Sci. Technol*. **2022**, 225, 109520.
9. Lu, Y.; Wang, J.; Wang, L.; Zhao, D.; Song, S. Construction of 3D Carbon Fiber/carbon Nanotube/silicone Rubber Nanocomposites for Stretchable Conductors Through Interface Host-guest Dendrimers. *Compos. Sci. Technol*. **2021**, 205, 108692.
10. Lin, Y.; Liu, S.; Peng, J.; Liu, L. Constructing a Segregated Graphene Network in Rubber Composites Towards Improved Electrically Conductive and Barrier Properties. *Compos. Sci. Technol*. **2016**, 131, 40-47.
11. Song, P.; Wang, G.; Zhang, Y. Preparation and Performance of Graphene/carbon Black Silicone Rubber Composites Used for

Highly Sensitive and Flexible Strain Sensors. *Sens. Actuators, A.* **2021**, 323, 112659.
12. Yang, Z.; Liu, H.; Wu, S.; Tang, Z.; Guo, B.; Zhang, L. A Green Method for Preparing Conductive Elastomer Composites With Interconnected Graphene Network via Pickering Emulsion Templating. *Chem. Eng. J.* **2018**, 342, 112-119.
13. Luo, S. D.; Liu, T. SWCNT/Graphite Nanoplatelet Hybrid Thin Films for Self-Temperature- Compensated, Highly Sensitive, and Extensible Piezoresistive Sensors. *Adv. Mater.* **2013**, 25, 5650-5657.
14. Segev-Bar, M.; Haick, H. Flexible Sensors Based on Nanoparticles. *ACS Nano* **2013**, 7, 8366-8378.
15. Tang, M.; Jiang, Z.; Wang, Z.; Qin, Y.; Jiang, Y.; Wu, L.; Li, Z. High-adhesion PDMS/Ag Conductive Composites for Flexible Hybrid Integration. *Chem. Eng. J.* **2023**, 451, 138730.
16. Zhang, H.; Liu, N.; Shi, Y.; Liu, W.; Yue, Y.; Wang, S.; Ma, Y.; Wen, L.; Li, L.; Long, F.; Zou, Z.; Gao, Y. Piezoresistive Sensor with High Elasticity Based on 3D Hybrid Network of Sponge@CNTs @Ag NPs. *ACS Appl. Mater. Interfaces* **2016**, 8, 22374-22381.
17. Huang, P.; Xia, Z.; Cui, S. 3D Printing of Carbon Fiber-filled Conductive Silicon Rubber. *Mater. Des.* **2018**, 142, 11-21.
18. Azizkhani, M. B.; Kadkhodapour, J.; Rastgordani, S.; Anaraki, A. P.; Shirkavand Hadavand, B. Highly Sensitive, Stretchable Chopped Carbon Fiber/Silicon Rubber Based Sensors for Human Joint Motion Detection. *Fibers Polym*. **2019**, 20, 35-44.
19. Yang, H.; Gong, L. H.; Zheng, Z.; Yao, X. F. Highly Stretchable and Sensitive Conductive Rubber Composites with Tunable Piezoresistivity for Motion Detection and Flexible Electrodes. *Carbon* **2020**, 158, 893-903.
20. Huang, P.; Xia, Z.; Cui, S.; Wang, J.; Zhao, S. Potential Temperature Sensing of Oriented Carbon-fiber Filled Composite and Its Resistance Memory Effect. *J. Mater. Sci.: Mater. Electron.* **2019**, 30, 9612-9622.
21. Li, Y.; Liu, G; Wang, L.; Zhang, J.; Xu, M.; Shi, S. Q. Multifunctional Conductive Graphite/cellulosic Microfiber-natural Rubber Composite Sponge with Ultrasensitive Collision-warning and Fire-warning. *Chem. Eng. J.* **2022**, 431, 134046.